Water Resour Manage (2008) 22:1051–1067
DOI 10.1007/s11269-007-9210-z

Flood Intensification due to Changes in Land Use

Bahram Saghafian · Hassan Farazjoo · Babak Bozorgy · Farhad Yazdandoost

Received: 2 October 2006 / Accepted: 9 July 2007 /
Published online: 28 August 2007

Abstract The non-stationarity in runoff regime may be attributed to various causes such as climate change, land use change, and man-made runoff control structures. Degradation of land use can induce significant impact on infiltration and surface roughness leading to higher flood discharges. This study aims at quantifying possible effects of land use changes and identifying flood source areas for future flood control planning in the Golestan watershed located northeast of Iran. A preliminary trend analysis on the annual maximum flood record of three stations inside the watershed showed that two stations were subject to anthropogenic change. This is while no trend could be detected in the annual maximum rainfall records in the region. Using a calibrated event-based rainfall-runoff model, flood hydrographs corresponding to land use conditions in 1967 and 1996 were simulated and relative changes in the peak flow of the two subsequent conditions were determined for different return periods. The results showed that the impact of land use changes on the flood peak discharge is considerably greater in some subwatersheds. Two limiting land use scenarios were also considered to investigate the envelope of future flood peaks in the watershed. By successively eliminating subwatersheds from the simulation process in a method titled "unit flood response", the contribution of each subwatershed to the outlet flood peak was quantified. Contribution, per unit area, to the outlet flood peak was the basis to rank the subwatersheds in terms of their flood potential.

B. Saghafian (✉)
Soil Conservation and Watershed Management Research Institute, 13445-1136, Tehran, Iran
e-mail: saghafian@scwmri.ac.ir

H. Farazjoo
Golestan Regional Water Company, 49139-33165, Gorgan, Iran
e-mail: farazjoo@yahoo.com

B. Bozorgy · F. Yazdandoost
K. N. Toosi University of Technology, Tehran, Iran

B. Bozorgy
e-mail: B.Bozorgy@wri.ac.ir

F. Yazdandoost
e-mail: Yazdandoost@kntu.ac.ir

Keywords Land use changes · Land use scenario · Flood · Flood source areas · Unit flood response · Rainfall-runoff model · HEC-HMS · GIS

1 Introduction

Soil, land cover, and topography are the three primary watershed characteristics that govern rainfall-runoff-erosion response in watersheds. Alteration of soil and topography is limited to small scales. Therefore, variation of watershed hydrologic response over time depends primarily on changes in the type and distribution of land cover (Miller et al. 2002). The hydrologic effects of land use and vegetation management are manifest in many ways such as water yield, low or high flow, soil moisture, and evapotranspiration (Sikka et al. 2003). The ability to predict the effects of changes in land use on streamflow and water quality is a valuable component in developing catchment management policies (Croke and Jakeman 2001).

While statistical trend analysis of recorded flood series is a valuable tool which may detect the non-stationarity in the hydrologic response of a watershed, it cannot quantify the change. Moreover, the trend tests are of limited use in the prediction phase and lump effect of land use and climate change. Experimental watersheds or hydrologic models are considered suitable tools in evaluation and prediction of hydrologic response variation. Although experimental watershed setup is considered appropriate in investigating the impact of land use change (Post 1996), it is difficult to use this approach to analyze hydrological time series from "real life" medium-sized (100–2,500 km^2) catchments (Lorup et al. 1998). Lorup et al. (1998) then recommended combined use of hydrologic models and traditional statistical tests, where data is available, to analyze the impact of land use on runoff.

Suwanwerakamtorn (1994) investigated the effect of upstream land use change on downstream flood pattern using HEC-1 model and geographic information system (GIS). Different scenarios were determined based on the basin forest area. The results showed that both main basin and sub-basin runoff increases as forest area decreases.

Miller et al. (2002) investigated the effect of land use and vegetation cover change on the hydrologic response of two basins in the United States by integrating hydrologic models and GIS. Analysis of runoff trend variation carried out by SWAT based on CN method showed that in San Pedro basin with the area of 3,150 km^2, average annual runoff increased due to the decrease in forest area and development in agricultural and urban areas between 1973 and 1997. The effect of land use change decreased as rainfall return period and duration increased.

Bahremand et al. (2006) applied the WetSpa model, presented earlier by Liu and De Smedt (2005) to predict flood hydrograph and the spatial distribution of hydrological characteristics in a watershed, for assessing reforestation impacts on floods in Margecany-Hornad watershed, Slovakia. The considered scenario involved a 50% increase of forest areas which resulted in 12% decrease in the peak discharge. Also, the time to peak of the simulated hydrograph of the reforestation scenario was 14 h longer than for the present land use. The results showed that the effect of land use on floods was strongly related to storm characteristics and antecedent soil moisture condition.

In general, the application of hydrologic models in land use change impact studies has received more attention in recent years. Ewen and Parkin (1996) stated that because of the success claimed by the reported studies on hydrological aspects of land use changes, it is likely that water resources managers will increasingly use computer models as a decision-making tool.

2 Motivation and Objectives

Beginning late evening on 10 August 2001 and continuing into the next day, an exceptionally heavy rainfall covered large areas in north and northeastern parts of Iran including Golestan Province. The rainstorm sparked a flood in the streams and rivers in the Golestan Dam watershed. The powerful flood traversed the basin, devastating essentially everything in its path. Trees, road guards, asphalt, large boulders, houses, automobiles, buses and trucks, heavy machinery, bridges, and, more importantly, human beings were removed and carried downstream by the flood into the Golestan Dam reservoir. While upstream hydrometric stations were mostly destroyed in the event leaving no record, the discharge into the reservoir was estimated at over 3,000 m^3/s based on the reservoir water level recorder. The flood claimed many lives and some missing. Many of the dead and missing people were tourists staying overnight in the Golestan forest. In addition to the death toll, thousands were left without homes and were evacuated to safety during the deluge. The floodwaters submerged some 10,000 ha of forest and pastureland and over 15,000 ha of valuable farmland. And last but not least, approximately 10% of Golestan Dam reservoir was filled with sediment only after 2 years of operation (Sharifi et al. 2002). Ironically, a smaller flood occurred in the same watershed in the same month of August in 2002 and caused some damages.

Following these flood events, a study was initiated to investigate whether past and future land use changes in the watershed may have increased, or will change, the flood hazard of Golestan watershed. Specifically, relative increase/decrease of the flood peaks is of primary interest. The study also attempts to identify flood source areas with respect to flood occurrence at the downstream reaches for further flood control planning. Land use maps corresponding to a 29-year period are prepared and HEC-HMS rainfall-runoff model is calibrated and applied to quantify the impact of past and future land use change on downstream flood peaks. The model is later used to determine the contribution of various subwatersheds on downstream flood peaks.

3 Description of Study Area and Data Analysis

Although the dominant climate in Iran is characterized as arid and semi-arid, the northern part of the country along the southern Caspian Sea coastline receives high to moderate precipitation. Annual precipitation, however, decreases in west–east direction. Golestan province is located in the eastern part of the southern Caspian Sea coastline. The Golestan watershed lies between 53°,13′ and 56°,28′ E longitude and 36°,57′ and 37°,46′ N latitude. The climate of this area is characterized as mild and the annual precipitation drops from 450 to 250 mm in west–east direction. The watershed drains 4,802 km^2 of land into the ~90 million cubic meters Golestan Dam reservoir. Luckily, the dam came into operation in 1999 just 2 years before the devastating 2001 great flood. Figure 1 shows the location of the watershed in the country and the boundary of three main subwatersheds.

Moderate range and bare lands cover the upper parts of Mother–Sou and Haji-Ghooshan subwatersheds. Forest areas, totaling about 1,240 km^2 in area, cover the middle parts of the watershed. In forested areas, the river valley is relatively narrow and steep. The downstream part of the watershed consists of mixed farm and rangeland, including large cotton and potato fields. Over the years, a portion of hillslope forest and rangelands has been turned into dry farming, producing excessive runoff and erosion.

Time series of the annual maximum 24-hr rainfall extracted from the records of existing raingage stations and the annual maximum flood (AMF) of three hydrometric stations located

Fig. 1 Location of Golestan Province and the study watershed in Iran

inside the watershed (Fig. 2) were collected and analyzed for possible trend. Kendall non-parametric test was performed to detect any trend in the data. The trend analysis showed no statistically significant trend in the rainfall data for the past 30 years. However, AMF series signaled a significant (1% level) trend at H2 and H3 stations. This may be attributed to the land use changes which have occurred upstream of these two stations.

A frequency analysis was also performed on the AMF series of the three hydrometric stations. The AMF record starts in year 1967. The first window of 15 years was positioned on 1967–1981 period and the second window covered 1986–2000. At this stage, it was assumed that the data in each 15-yr window is stationary. The huge flood of 2001 was not included in the analysis since the discharge estimation was not reliable. Then for each window, the 5-yr flood magnitude was estimated based on the best probability distribution function. A clear increase in the 5-yr flood was observed at H2 and H3 stations such that the 5-yr flood of 1986–2000 window had increased by over 50% compared with that of 1967–1981 window. This bold increase underlines the effect of anthropogenic effects on runoff series in the absence of rainfall trends.

4 Materials and Methods

4.1 Landscape Characterization and GIS Applications

The Golestan watershed can be divided into 11 main subwatersheds denoted by B1 to B11 (Fig. 2). Ten intermediate subwatersheds are also identified which are referred to by IB1 to IB10. The size of main subwatersheds ranges from 110 to 595 km^2. Although only three hydrometric stations exist in the whole watershed and thus the response of all main subwatersheds cannot be individually checked, a relatively detailed subwatershed delineation scheme had to be selected in order to study the relative change in floods attributed to land use changes and to carry out the flood source analysis in smaller units.

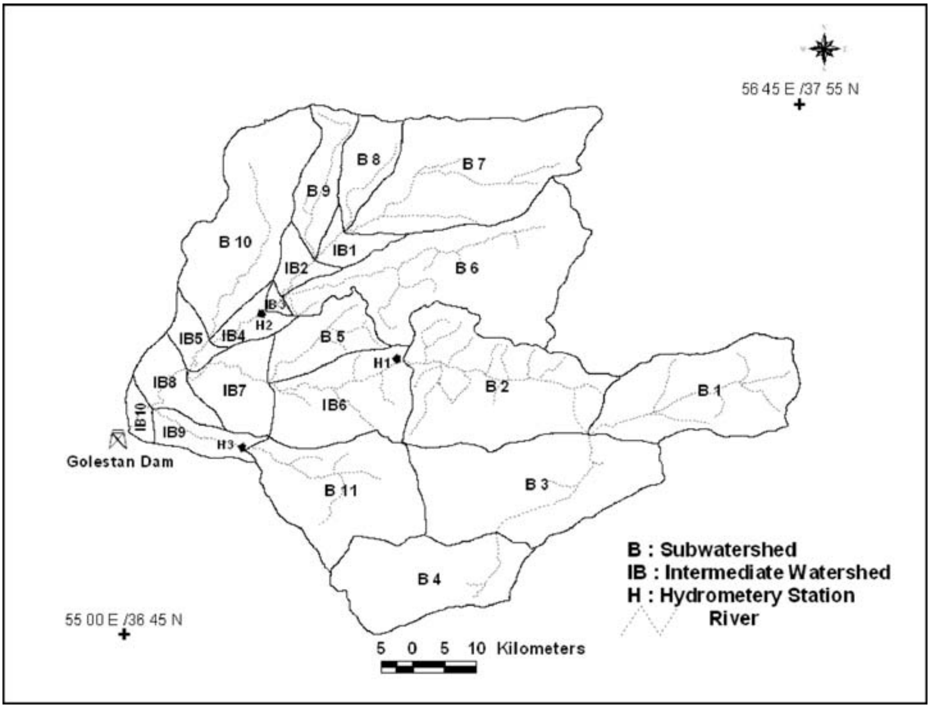

Fig. 2 Golestan subwatershed boundaries and location of hydrometric stations

Thus, it is implicitly assumed that the calibration of several subwatersheds contained within the drainage area of each hydrometric station is a valid practice.

The digital elevation model (DEM) of the basin was prepared in the GIS with a 50-meter pixel size based on 1:50,000 topographic maps (Fig. 3). The physiographic characteristics of all subwatersheds were derived from the DEM and are summarized in Table 1.

Available 1967 1:25000 land use paper map of Golestan watershed was digitized in the GIS. The land use map of 1996 had been prepared in another study based on Landsat TM images and field inspections. Figures 4 and 5 show the land use maps of 1967 and 1996, respectively. These figures demonstrate that land use has undergone substantial degradation due to expansion of agricultural lands over hill slopes and overgrazing of rangelands. Available map of hydrologic soil groups was also imported into the GIS. About 68% of the watershed area consists of class C and 22% consists of class B soil groups.

4.2 Rainfall-Runoff Model

In this study, HEC-HMS model was selected to simulate the hydrologic response of the watershed. HMS is a computer model that includes several options for infiltration, runoff routing, base flow, and river routing. The model consists of three main sections, namely basin model, meteorologic model and control specifications. HMS model is capable of automatic parameter calibration (USACE 2000).

To account explicitly for land use and soil type, SCS curve number (CN) method was used to determine infiltration. SCS unit hydrograph was also selected for excess rainfall-

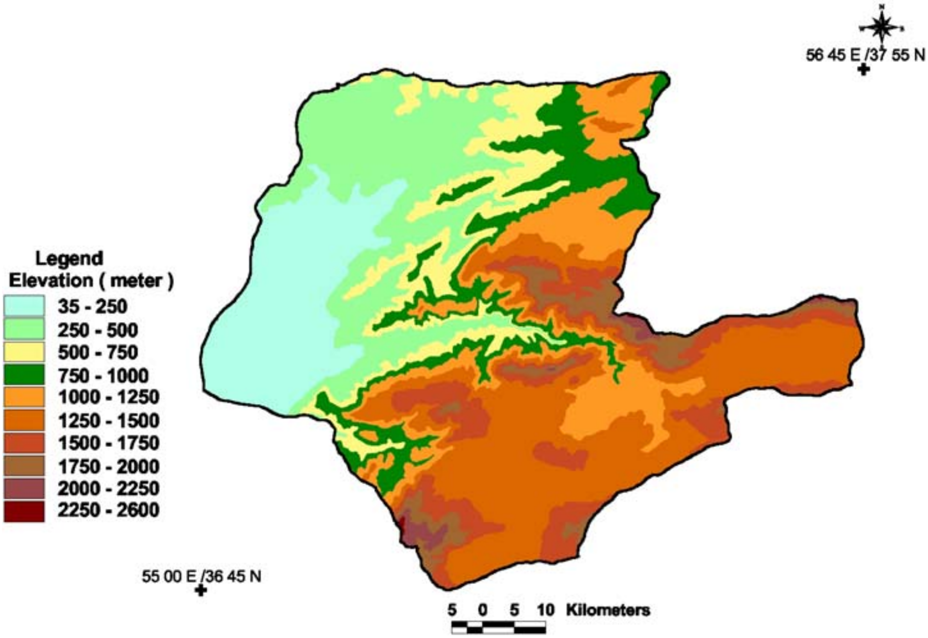

Fig. 3 DEM of Golestan watershed

runoff transformation. Flood routing from the outlet of subwatersheds to the main outlet was carried out by the Muskingum method. In order to develop the CN maps corresponding to 1967 and 1996 years, hydrologic soil group map was overlaid by the land use maps in the GIS environment. The CN of each sub-basin was then determined by the weighted average method.

For calibration and validation of HMS, flood hydrographs recorded at H1, H2, and H3 hydrometric stations and the corresponding rainfall events measured at some 12 rain gauge stations in the Golestan watershed were collected. Many of the rainfall-runoff events had to be discarded due to incomplete simultaneous rainfall and runoff records. The spatial distribution of rainfall events was determined based on the inverse distance squared method. The simple-split sample test method was applied to calibrate and subsequently validate HEC-HMS (Ewen and Parkin 1996). Observed floods were classified into two groups. Model parameters were calibrated based on the first data group with percent error in peak discharge as the criteria and then validated against the second data group. In all, three events were used for calibration and two for validation at each station. All events fell in class I of CN Antecedent Moisture Condition (AMC) and their record dates were within 5 years before or after 1996.

The subwatershed average CN value was determined based on the CN map and was kept constant during the calibration. Initial loss ratio and lag time were calibrated for subwatersheds. The Muskingum K was determined for each river reach based on the cross section geometry, while Muskingum X was set at 0.2. Calibration results showed that the lag time calculated by the SCS empirical formula was slightly different from the calibrated lag time. Ignoring the small differences, the lag time calculated by SCS formula was used for all subwatersheds. The calibrated initial loss, in the range of 0.05S to 0.15S (S is the water storage capacity of the soil), was assumed uniform for each CN class. The subwatershed lag time values varied from 1 to 10.5 h.

Table 1 Physiographic characteristics of Golestan main subwatersheds

Subwatershed code	Subwatershed name	Area(km^2)	Watershed mean slope (%)	Mean elevation(m)	Mean river slope (%)	Main river length (km)
B1	Rebat-e-Gharebil	383	7.6	1,468	1.2	33.5
B2	Tangrah	498	22.0	1,321	3.9	37.3
B3	Dasht-e-Daniyal	509	6.5	1,379	1.3	18.5
B4	Nardin	332	8.0	1,608	1.5	10.2
B5	Yekkeghooz	141	16.4	623	3.6	22.2
B6	Yalcheshmeh	595	12.6	1,044	1.4	46.8
B7	Gharnaveh	495	10.3	790	3.3	29.9
B8	Shoordareh	110	6.2	456	1.9	21.8
B9	Hajibeyk	120	5.6	392	1.6	31.0
B10	Yaramtapeh	409	3.3	279	1.1	37.8
B11	Galikesh	372	16.7	1,255	4.2	22.7
IB1	–	54	12.6	455	1.1	9.0
IB2	–	52	3.8	233	1.1	0.2
IB3	–	12	6.7	258	0.4	8
IB4	–	57	5.5	210	0.2	16.2
IB5	–	51	0.2	102	0.1	10.2
IB6	–	269	17.8	830	1.1	12
IB7	–	143	3.9	197	0.4	23.3
IB8	–	91	0.6	97	0.4	10.2
IB9	–	78	7.2	244	1.1	17.4
IB10	–	30	0.9	56	0.4	7.1
Watershed	Golestan Watershed	4802	10.6	953	1.3	123.2

The absolute error in peak discharge in calibration and validation stages varied in 0–5 and 3–12 percent range, respectively. The highest peak discharge of all events was under 250 m^3/s at H3. The model generally overestimated the validation events. Since no complete runoff hydrograph record of larger events was available for calibration/validation, it was assumed that the model's simulation results corresponding to high return periods are valid in relative terms, i.e. for comparison of the relative difference in peak discharges due to past or future land use conditions.

4.3 Past Land Use Changes and Future Land Use Scenarios

Land use changes from 1967 to 1996 were studied for each subwatershed using GIS. The results indicate that conversion of rangelands to agriculture is the major land use change in the watershed. The total area of cultivated lands has increased non-uniformly across the subwatersheds. B8 and B9 subwatersheds have undergone the most substantial changes with 46% and 34% increase in agricultural area, respectively. Table 4 summarizes the area changes in each land use category from 1967 to 1996 over the watershed (Table 2).

Two limiting future scenarios, one optimistic and another pessimistic, were considered for predicting the upper and lower thresholds of variation of hydrologic response in the watershed. The 1996 land use map was considered as the initial condition to develop both scenarios in GIS. The trend in deterioration of vegetation cover is considered as in Table 3 for the pessimistic scenario. In the optimistic scenario, it was assumed that the proposed land use management plan is to be carried out. This implies that the rangelands condition is upgraded by keeping the sheep out of the land. Moreover, trees are to be planted in low-density forest areas and hillslope cultivated lands change to orchards. In the revised land

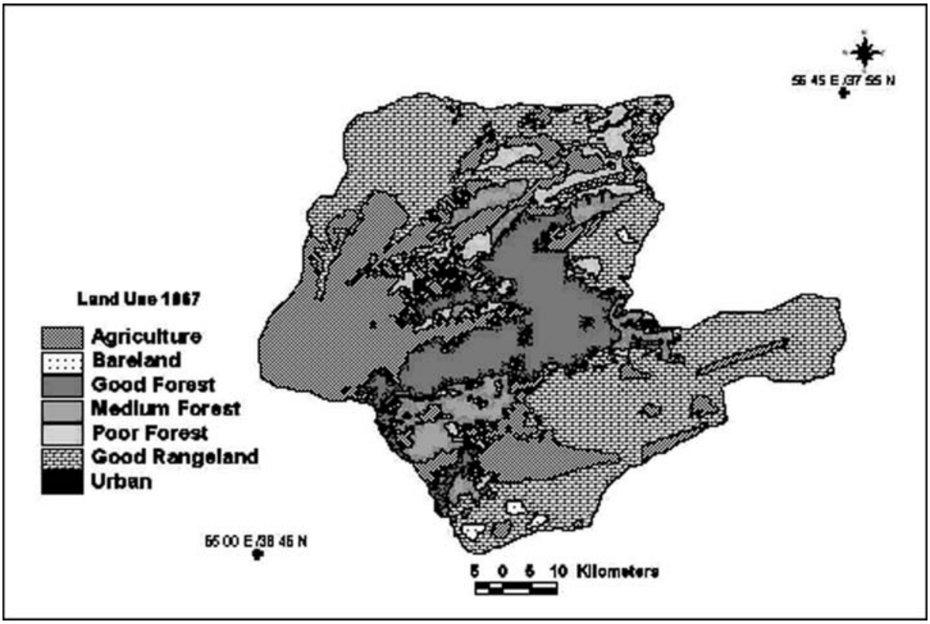

Fig. 4 Land use map of Golestan watershed in 1967

use plan drafted after the great flood in summer 2001, some 37,200 ha of sloped cultivated lands in hilly areas are to be converted into olive and walnut orchards. Table 4 shows the land use condition in the optimistic scenario.

4.4 Effect of Land Use Changes on Flood Peak

The HMS model was used to predict land use effects on floods of Golestan watershed for various design rainfall conditions. First, maximum daily rainfall depths measured at stations inside and adjacent to Golestan watershed were statistically analyzed and daily storm depths corresponding to different return periods were estimated. The spatial distribution of design rainfalls was determined based on the inverse distance squared method. Rainfall hyetographs were made to follow the average temporal pattern of a recording raingage in the area.

The model was run for the 1967 and 1996 land use conditions as well as for the optimistic and pessimistic scenarios. The changes in peak discharge and volume as a result of changes in the land use in the watershed were then analyzed. The results are discussed in "Section 5."

4.5 Identification of Flood Source Areas

One of the most important tasks in flood control planning is the identification of flood source areas. Such areas must be ranked with respect to their effects on areas subject to flood damage, which are usually concentrated closer to the outlet. We used the "unit flood response" approach proposed by Saghafian and Khosroshahi (2005) to rank different subwatersheds with respect to their contribution to the flood generation at downstream watershed areas. In the unit response approach, the total discharge at the main outlet is

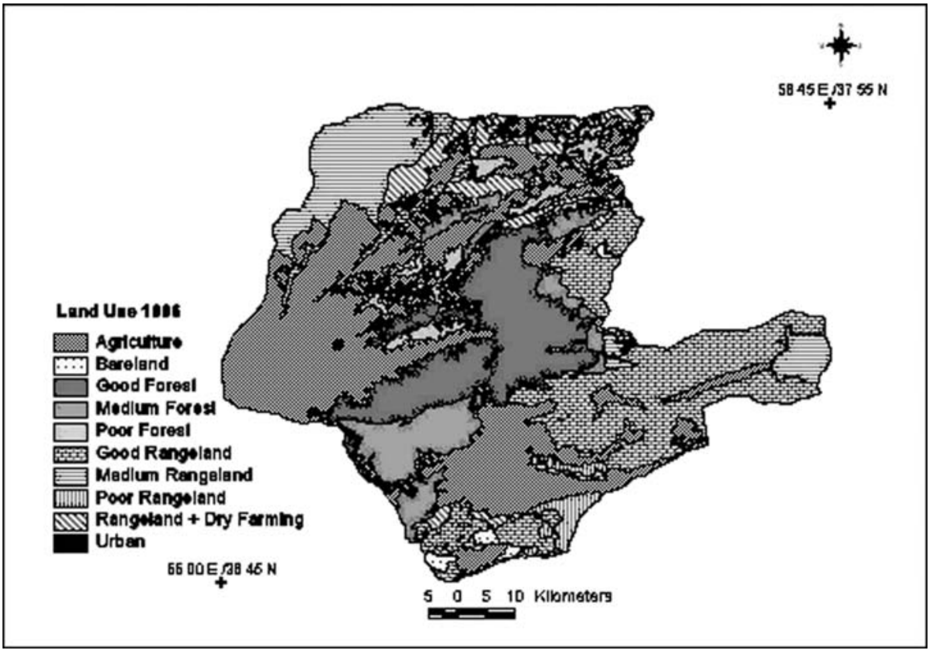

Fig. 5 Land use map of Golestan watershed in 1996

determined after successively eliminating each subwatershed in the process of river flood routing. Thus, the contribution of each subwatershed on the flood peak at the outlet is disaggregated. The subwatershed with the largest decrease on the flood peak is given the highest flood rank. Other subwatersheds may also be ranked based on their contribution. Two flood indices are defined as follows:

$$F = (\Delta Q_P / Q_P) * 100 \tag{1}$$

$$f = \Delta Q_p / A \tag{2}$$

where F (%) and f ($m^3/s/km^2$) are gross and per unit area flood indices, respectively, ΔQ_P is the amount of reduction in peak discharge due to elimination of the subwatershed (m^3/s),

Table 2 Land use change in Golestan watershed from 1967 to 1996

Land use category	1967		1996		Change (%)
	Area (km^2)	Area (%)	Area (km^2)	Area (%)	
Agriculture	1,361.4	28.3	1,988.6	41.4	+13.1
Bare land	27.0	0.56	36.2	0.75	+0.19
Good forest	745.6	15.52	657.1	13.68	−1.84
Medium forest	381.4	7.94	376.1	7.83	−0.11
Poor forest	310.2	6.45	210.7	4.38	−2.07
Rangeland	1,975.7	41.13	1,529.7	31.85	−9.28
Urban	1.4	0.03	3.6	0.07	+0.04
Total	4802.7	100	4802.7	100	–

Table 3 Land use condition in the pessimistic scenario

1996 Land use	Pessimistic land use scenario
Good forest	Medium forest
Medium forest	Poor forest
Poor forest	Agriculture
Good/Medium rangeland	Poor rangeland
Agriculture	Agriculture
Rangeland+Dry Farming	Agriculture

Q_p is the total peak discharge (m^3/s), and A is the subwatershed area (km^2). HMS was applied to determine the flood index values corresponding to 1996 land use conditions based on the 50-yr 24-h design rainfall. The station values of rainfall were spatially distributed over the watershed using inverse squared distance method.

5 Results and Discussion

The effect of different land use conditions on the outflow peak discharge is investigated for storms with return periods from 5 to 1,000 years. Table 5 and Fig. 6 show a comparison between the outflow peak and the total flood volume of the basin corresponding to 1967 and 1996 land use conditions.

Comparison of the Golestan watershed land use maps of 1967 and 1996 shows that forest and rangelands have been converted into cultivated areas. The area of cultivated lands has risen by 13%, which mostly occurred on hillslopes. During the same period, the total forest area has decreased from 1,437.2 to 1,243.9 km^2, i.e. a reduction of about 200 km^2 (4% of the total watershed area). The model simulations show that, for a given return period, flood peak and total flood volume increased from 1967 to 1996 as a result of forests and rangelands being converted into cultivated areas. However, change in the flood peak and flood volume differs in different subwatersheds because of non-uniform land use changes. The smallest change is observed in B2, which mainly consists of Golestan Forest protected area. The largest flood peak changes occur in B7, B8, B9 and B10 subwatersheds where a great portion of rangelands has been converted into cultivated areas.

The largest and smallest relative effect due to land use changes from 1967 to 1996 occurred in B8 and B2 subwatersheds with 161% and 8% increase in the 5-year flood peak, respectively. This is while during the same period, the 5-year flood peak of the whole

Table 4 Land use improvement plan in the optimistic scenario

1996 Land use	Optimistic land use scenario
Good forest	Good forest
Medium forest	Good forest
Poor forest	Medium forest
Good rangeland	Good rangeland
Medium rangeland	Good rangeland
Poor rangeland	Medium rangeland
Rangeland+dry farming	Medium rangeland
Agriculture – slope over 10%	Orchard
Agriculture – slope under 10%	Agriculture with soil conservation

Table 5 Changes in flood peak and volume for different return periods

Return period (yr)	Peak flow (m^3/s)			Flood volume (MCM)		
	1967	1996	Percent change	1967	1996	Percent change
5	477	628	31.7	30.7	39.5	28.7
10	701	902	28.5	45.5	57.2	25.7
25	104	1,302	25.0	68	83.6	22.8
50	1,332	1,640	23.1	87.6	106.0	21.1
100	1,656	2,015	21.6	109.2	130.7	19.6
200	2,011	2,420	20.3	133.4	157.8	18.3
500	2,531	3,008	18.8	169.0	197.6	16.9
1,000	2,966	3,494	17.8	199.0	230.6	15.9

watershed increased by 31.7%. As expected, the relative effect of land use change decreases in flood events of higher return periods. For example, land use changes from 1967 to 1996 have caused a 31.7% increase in the 5-yr flood peak but only a 18.8% increase in the 100-yr flood peak.

Flood peaks were also simulated for B1 to B10 subwatersheds in optimistic and pessimistic land use scenarios. The results are presented in Table 6 and Fig. 7. The comparison between optimistic and pessimistic scenarios shows that these two land use conditions almost mirror each other with respect to the 1996 condition as far as the change in the flood peak of Golestan watershed is concerned. In other words, if land cover goes through a deteriorating trend towards pessimistic scenario conditions, the flood peak will increase by almost the same percentage as optimistic scenario can cause reduction of the

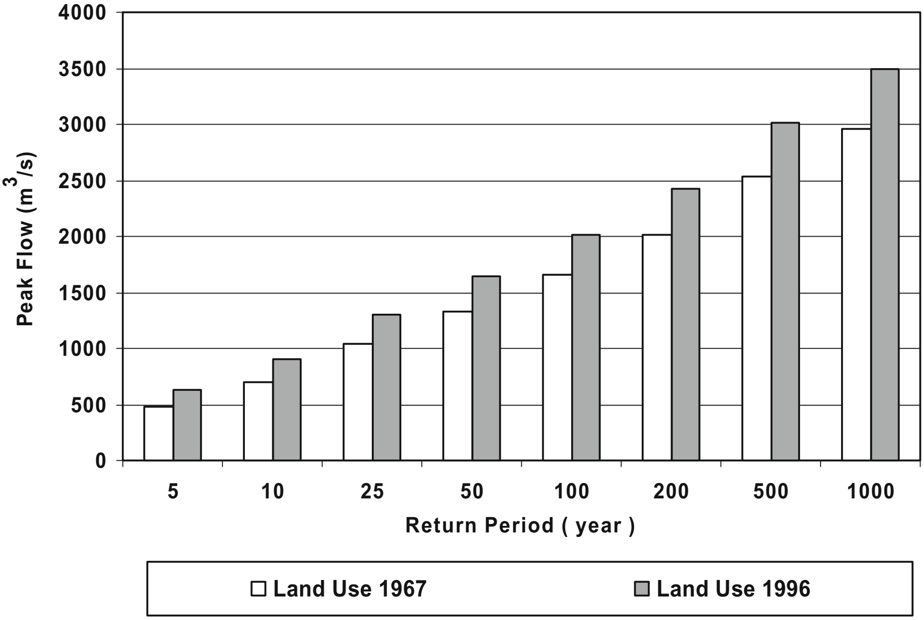

Fig. 6 Comparison of peak outflow for different return periods corresponding to 1967 and 1996 land use conditions

Table 6 Flood peaks for different return periods in pessimistic and optimistic land use scenarios

Return period (yr)	Peak flow (m^3/s)			Percent change of pessimistic scenario over 1996 condition	Percent Change of optimistic scenario over 1996 condition
	Current land use(1996)	Pessimistic scenario	Optimistic scenario		
5	628	850	436	35.5	−30.5
10	902	1,188	647	31.9	−28.2
25	1,302	1,673	968	28.5	−25.7
50	1,640	2,070	1,244	26.2	−24.1
100	2,015	2,502	1,553	24.2	−22.9
200	2,420	2,964	1,893	22.5	−21.8
500	3,008	3,633	2,393	20.8	−20.4
1,000	3,494	4,185	2,811	19.8	−19.5

peak values. The rate of change reduces for higher return periods as expected since the role of land use effect shrinks for higher intensity storms. Considerable peak reduction for low to intermediate return periods highlights the importance of land cover rehabilitation planned in the optimistic scenario. For instance, the flood peak for a 100-year return period in optimistic scenario will decrease by 23% in comparison to the 1996 condition.

Table 7 and Figs 8, 9, 10, and 11 show ranking of B1 to B11 subwatersheds in terms of different flood characteristics. Note that the last column of Table 7 indicates the ratio of rainfall depth received by each subwatershed over the spatially averaged watershed value. According to Table 7 (column 3) and Fig. 8, B11 subwatershed produces the largest subwatershed flood peak by 308.8 m^3/s. B1 subwatershed, however, generates the smallest subwatershed peak by 23.4 m^3/s.

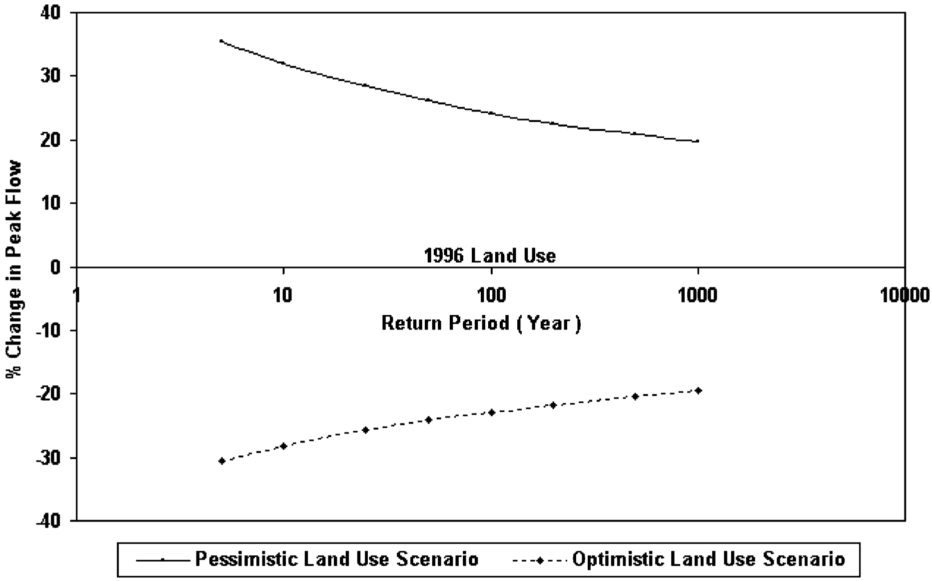

Fig. 7 Flood peak envelope created by optimistic and pessimistic scenarios

Table 7 Comparison of subwatershed 50-yr flood peak generation

Subwatershed(1)	Area (km^2)(2)	Peak discharge (m^3/s)(3)	Outlet peak discharge without subwatershed (m^3/s)(4)	Peak discharge reduction(m^3/s)(5)	*F* (%) (6)	*f*(m^3/s / km^2) (7)	Priority based on column (3) (8)	Priority based on F(9)	Priority based on f(10)	Ratio of rainfall in subwatershed over entire watershed (11)
B1	383.3	23.4	1,628.3	11.9	0.72	0.03	11	11	11	0.52
B2	498.9	140.9	1,522.2	118	7.19	0.24	7	5	9	0.93
B3	509.5	173.4	1,494.9	145.3	8.86	0.29	3	3	6	0.9
B4	331.9	152.0	1,493.5	146.7	8.94	0.44	5	2	2	1.0
B5	141.2	52.9	1,588.8	51.4	3.14	0.36	9	8	3	1.02
B6	595.2	159.8	1,548.8	91.4	5.57	0.15	4	7	10	0.91
B7	495.5	197.5	1,502.2	138	8.41	0.28	2	4	7	0.9
B8	109.5	48.2	1,606.9	33.3	2.03	0.30	10	10	5	0.96
B9	119.9	55.9	1,600.9	39.3	2.4	0.33	8	9	4	1.0
B10	409.1	151.0	1,530.7	109.5	6.68	0.27	6	6	8	0.99
B11	372.5	308.8	1,404.2	236	14.4	0.63	1	1	1	1.33
Basin	4,802.7	1,640.2	–	–	–	–	–	–	–	1

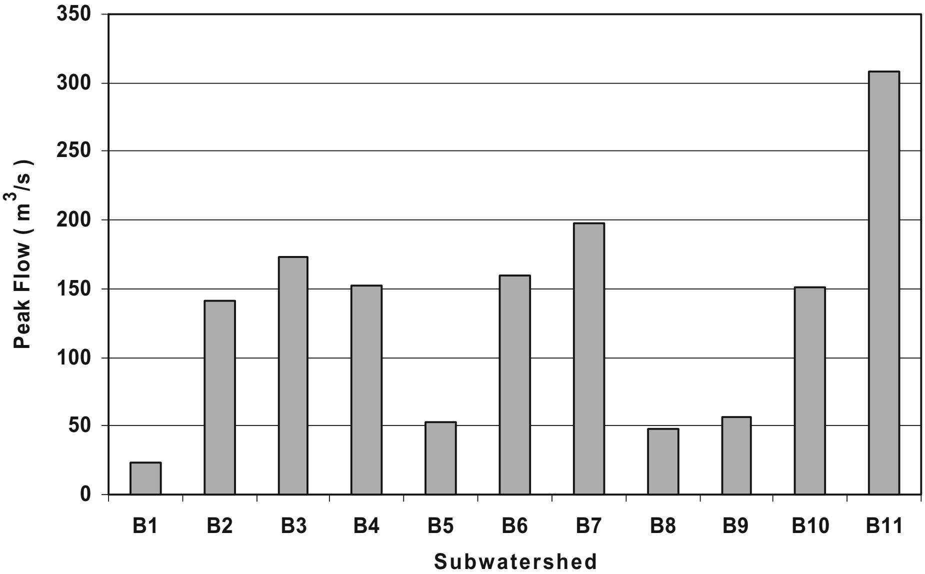

Fig. 8 Comparison of subwatershed peak discharge

However, based on the unit response approach, the flood source areas (i.e., subwatersheds) must be identified and ranked based on the values given in columns 6 (*F* flood index) and 7 (*f* flood index) of Table 7, as shown in Figs. 9 and 10. For instance,

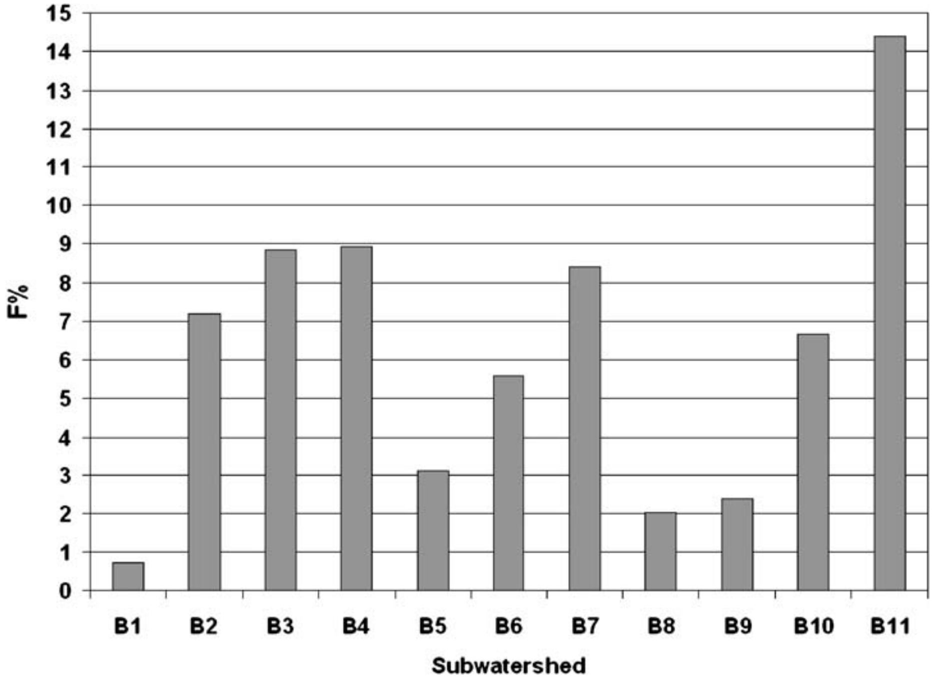

Fig. 9 Comparison of subwatershed F flood index

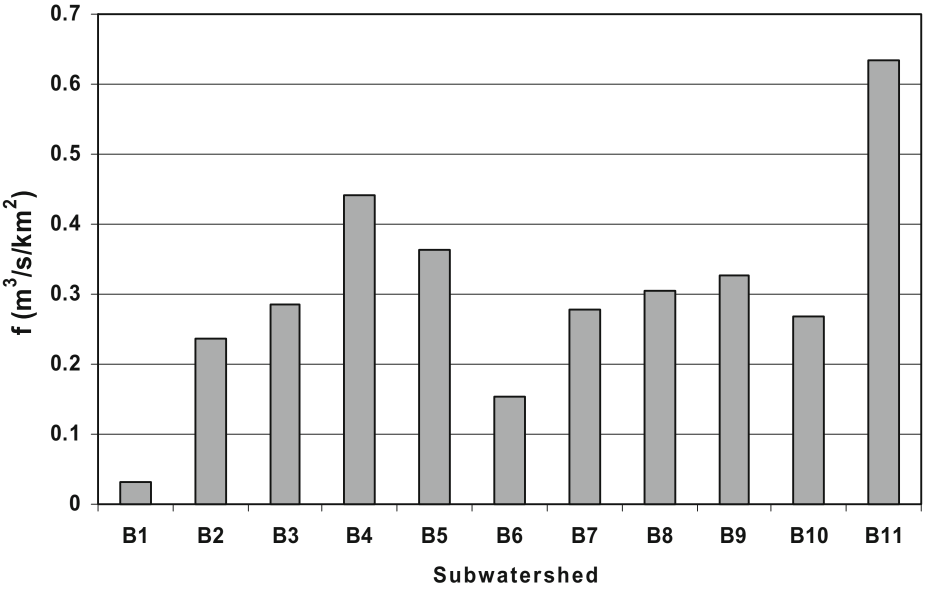

Fig. 10 Comparison of subwatershed *f* unit area flood index

the rank of B4 subwatershed, which is the eighth largest and has the fifth highest peak, jumps to the second position as far as F and f indices are concerned. This example underlines the integrated effect of different factors such as river routing, subwatershed location in the entire watershed, topology of river network, spatial distribution of rainfall, and also the subwatershed physical characteristics in determining the contribution of different areas on the outlet discharge. Such integrated effects can be simulated using hydrologic models. Since the subwatershed area is a deciding factor in flood control costs, the use of f index is preferred (columns 7 and 10 of Table 7). Figure 10 shows the flood potential ranking based on 'f' index where B11 is rated first and B1 is rated last. The flood index map is also depicted in Fig. 11 where only main subwatersheds are ranked.

Since the effect of location and other factors, particularly the rainfall spatial distribution, were incorporated in the "unit flood response" approach, it is evident that the peak flow generated by this subwatershed is well synchronized in terms of hydrograph timing with the flow of other areas. This has given B11 the highest flood index value. On the other hand, B1 and B6 subwatersheds produce small flood index values. The former receives relatively low rainfall but enjoys good rangeland and the latter has a low CN value.

6 Conclusions

In this study, the relative effect of land use change was quantified through simulating the flood hydrographs of Golestan watershed using a hydrologic model. The simulation results indicate that land cover deterioration has increased the flood peak and volume. Such effect on the hydrologic response is more pronounced in some of the subwatersheds. However, vegetation cover is not as effective in decreasing great floods with high return periods. The simulation results also imply that flood peak was more sensitive to land use change in comparison to flood volume. Olive and walnut planting have been proposed to improve land use condition of

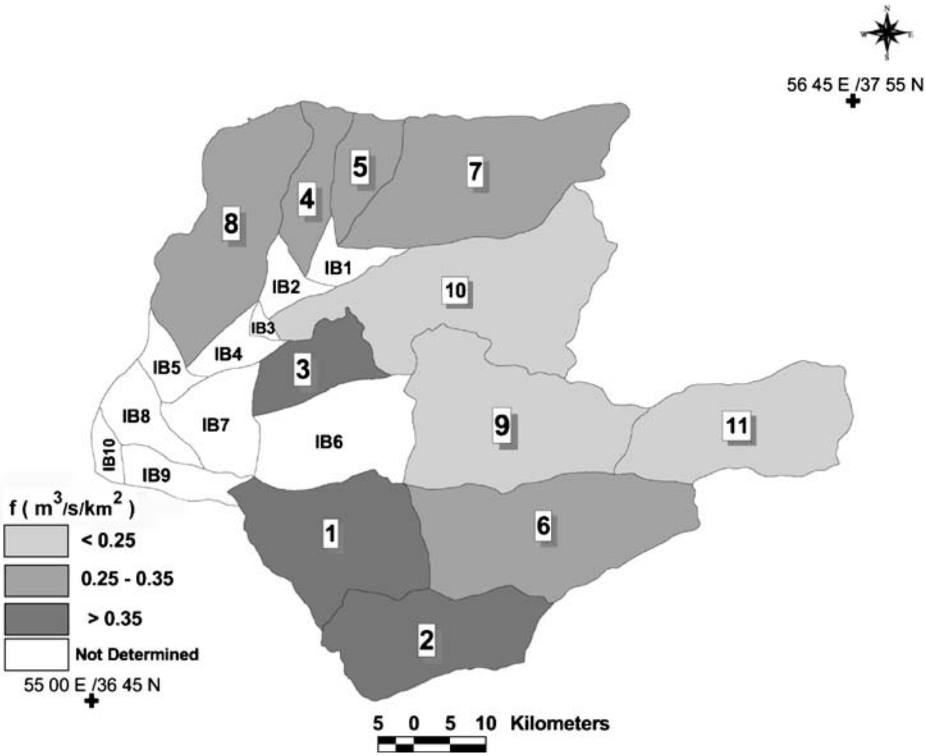

Fig. 11 Flood index ranking map of main subwatershed (*numbers* indicate the rank)

Golestan watershed in the context of an optimistic scenario. Although the motivation behind this scenario was not limited to flood control, it significantly reduces the flood peaks of low to moderate return periods. On the other hand, another extreme pessimistic land use condition greatly increases the flood hazard of the watershed. Comparison between the simulation results of optimistic and pessimistic scenarios shows that these two scenarios have similar favorable and unfavorable impacts on the flood peak of Golestan watershed, respectively. Considerable peak flood reduction for low to intermediate return periods highlights the effectiveness of land cover rehabilitation planned in the optimistic scenario.

Application of "unit flood response" approach shows that the B11 subwatershed not only produces the highest peak discharge at its own outlet, but also has the greatest contribution to the total peak discharge at the watershed outlet. Inspection of recorded flood data at H3 station located at the outlet of B11, confirms that this subwatershed is quite active in runoff generation with the highest specific discharge peaks of the hydrometric stations. Rainfall records of the raingauge station in this subwatershed are also considerably greater compared to the other stations.

In summary, this study integrated various tools such as hydrologic models, GIS, and remotely sensed data to assess the effect of past land use changes and predict the effect of future land use scenarios on the flood regime of Golestan watershed. The unit response technique was also capable of identifying and ranking various subwatersheds in terms of their flood contribution at the outlet. The results of such studies are quite helpful in flood control projects and assessment of flood characteristics of watersheds corresponding to land use scenarios.

List of Symbols:

A Subwatershed area (km^2)
F Gross flood index (in %)
F Unit area flood index ($m^3/s/km^2$)
Q_p Peak discharge (m^3/s)
ΔQ_P Reduction in peak discharge due to elimination of the subwatershed (m^3/s)

References

Bahremand A, De Smedt F, Corluy J, Liu YB, Poorova J, Velcicka L, Kunikova E (2006) WetSpa model application for assessing reforestation impacts on floods in Margecany-Hornad watershed. Water Resources Management, Slovakia

Croke BFW, Jakeman AJ (2001) Predictions in catchment hydrology: an Australian perspective. Mar Freshwater Res 52:65–79

Ewen J, Parkin G (1996) Validation of catchment models for prediction land use and climate change impacts: 1. Method. J Hydrol 175:583–564

Liu YB, De Smedt F (2005) Flood modeling for complex terrain using GIS and remote sensed information. Water Resour Manag 19(5):605–624

Lorup JK, Refsgaard JC, Mazvimavi D (1998) Assessing the effect of land use change on catchment runoff by combined use of statistical tests and hydrological modelling: case studies from Zimbabwe. J Hydrol 205:147–163

Miller SN, Kepner WG, Mehaffey MH, Hernandez M, Miller RC, Goodrich DC, Devonald K, Heggem DT, Miller WP (2002) Integrating landscape assessment and hydrologic modeling for land cover change analysis. J American Water Resour Assoc 38(4):915–929

Post DA (1996) Identification of relationships between catchment-scale hydrologic response and landscape attributes, PhD Thesis. Australian National University, Australian

Saghafian B, Khosroshahi M (2005) Unit response approach for priority determination of flood source areas. J Hydrol Eng 10(4):270–277, ASCE

Sharifi F, Saghafian B, Telvari A (2002) The Great 2001 Flood in Golestan Province, Iran: causes and consequences. International Conference on Flood Estimation, Switzerland

Sikka AK, Sarma JS, Sharda VN, Samraj P, Lakshmanam V (2003) Low flow and high flow responses to converting natural grassland into bluegum (Eucalyptus Globulus) in Nilgiris watersheds of South India. J Hydrol 270:12–26

Suwanwerakamtorn R (1994) GIS and hydrologic modelling for the management of small watersheds. ITC Journal 4:343–348

USACE (2000) HEC-HMS Technical Manual, Hydrologic Engineering Center. Davis, CA, 187 p